

Efficient radiative transfer modelling with SKIRT

Maarten Baes

European Southern Observatory, La Casilla 19001, Santiago 19, Chile

Sterrenkundig Observatorium, Universiteit Gent, Krijgslaan 281 S9, B-9000 Gent, Belgium

`mbaes@eso.org, maarten.baes@ugent.be`

and

Herwig Dejonghe

Sterrenkundig Observatorium, Universiteit Gent, Krijgslaan 281 S9, B-9000 Gent, Belgium

`herwig.dejonghe@ugent.be`

and

Jonathan I. Davies

Cardiff University, 5 The Parade, Cardiff CF24 3YB, Wales

`jonathan.davies@astro.cf.ac.uk`

ABSTRACT

We present SKIRT, a three-dimensional Monte Carlo radiative transfer code developed to study dusty galaxies. We discuss SKIRT's most important characteristics and present a number of applications. In particular, we focus on the kinematical aspect of SKIRT. We demonstrate that dust attenuation mimics the presence of dark matter around elliptical galaxies and that it severely affects the rotation curves of edge-on galaxies.

1. Introduction

In many astronomical situations dust plays a crucial role in our interpretation of observations. In these situations the inferences made from data may require accurate modelling of dust absorption, scattering and/or emission mechanisms. This modelling is not straightforward and is often neglected in the hope that it is not important. Only during the past few years, radiative transfer codes have become powerful enough to handle realistic two- or three-dimensional geometries. Many different approaches exist to handle the radiative transfer problem, and various authors have

adopted different techniques to study the effect of dust on the photometry and SEDs of galaxies (e.g. (14), (47), (15), (27), (45), (11), (40), (37), (10), (3), (4), (34), (21)). In this contribution, we present a three-dimensional Monte Carlo radiative transfer code SKIRT (Stellar Kinematics Including Radiative Transfer). The code was initially developed to study the observed kinematics of dusty galaxies, but it has now turned into a very flexible and general tool to study various radiative transfer problems in dusty systems.

2. Basic characteristics of SKIRT

The basic characteristics of Monte Carlo radiative transfer are described in e.g. (16), (32), (46), (20), (11), (24) and (35). The key ingredient in Monte Carlo radiative transfer is that the radiation field is treated as a flow of a finite number of monochromatic photon packages. At each moment in the simulation, a photon package is characterized by a luminosity, a frequency, a position and a propagation direction. A Monte Carlo radiative transfer simulation consists of consecutively following the individual path of each single photon package through the interstellar medium. The trajectory of the photon package is determined by various events such as emission, absorption and scattering events. Each event is generated randomly from the appropriate probability distribution. At the end of the simulation, knowledge of the individual path of each photon package is used to completely determine the radiation field at all positions, in all directions and at all frequencies.

Monte Carlo codes are very flexible, they allow arbitrary geometries for stars and dust and they are easy to interpret and to implement. The main disadvantage is also well-known: Monte Carlo codes are relatively slow and numerically demanding compared to other techniques. Our experience is, however, that this disadvantage is negligible compared to the benefits of the method, especially as Monte Carlo simulations can nowadays be optimized substantially by the inclusion of deterministic elements. Many of these elements are implemented into the SKIRT code, such as the forced first scattering principle (16), the peel-off technique (51) and continuous absorption (30). A novel and very useful feature is the frequency distribution adjustment principle introduced by Bjorkman & Wood (12). This powerful technique ensures that at each moment during a Monte Carlo simulation, the dust temperature and the local radiation field are always in agreement. As a result, Monte Carlo simulations can self-consistently calculate the dust temperature distribution and the far-infrared emission of galaxies without the costly iteration that is a necessary ingredient in most radiative transfer schemes. For a critical discussion, we also refer to (9). Apart from these optimization techniques borrowed and adapted from other Monte Carlo modellers, we have included two novel mechanisms in the SKIRT code: the use of partly polychromatic photon packages and the inclusion of kinematic information.

3. Polychromatic photon packages

The photon packages used in most Monte Carlo simulations are monochromatic, i.e. they consist of a unspecified number of individual photons with the same frequency. This has a good reason: many of the probability functions which determine the trajectory of a photon package are frequency-dependent. For example, the probability distribution of the covered path length before an interaction is an exponential distribution in optical depth space, and therefore a frequency-dependent distribution in physical path length. Consequences of this monochromatism are a low signal-to-noise of the radiation field in frequency regions where the stars and/or dust are only poor emitters and a noisy dust temperature distribution. SKIRT works with polychromatic photon packages, i.e. packages characterized by a continuous frequency distribution rather than by a single frequency. The photon packages are only partly polychromatic: they are polychromatic when they are emitted (by either the stars or the dust grains), but loose their polychromatism during a scattering event. In combination with the peel-off technique and the treatment of absorption as a continuous process, this mechanism assures that every single photon package contributes at least once to the observed radiation field at every single wavelength, and that the absorption rate is determined with much greater precision. As a result, much less photon packages (and thus CPU time) are necessary to obtain high signal-to-noise results.

4. The inclusion of kinematic information

Kinematical information on external galaxies is obtained from extracting line-of-sight velocity information from spectra, through measuring the Doppler shifts of either absorption lines (stars) or emission lines (gas). Often these spectra are taken in the optical regime and therefore they are subject to dust attenuation. The effect of dust attenuation on the observed kinematics is still largely unexplored. Most studies focused on the effect of dust absorption on the rotation curves of spiral galaxies ((17), (13), (31), (52), (43)). In order to investigate in a more general way how the observed kinematics of galaxies are affected by dust attenuation (including scattering), we have included the possibility to include kinematical information in the SKIRT code. This is accomplished by assigning to each photon package an additional characteristic: the line-of-sight velocity it carries with it. This characteristic is initialized according to the emitting star's velocity, and is updated during every scattering event. Note that this is not a trivial process because the individual velocities of both the stars and the scattering dust grains need to be taken into account. In order to increase the efficiency of the Monte Carlo simulation, we implemented a similar technique as the polychromatic photon packages: instead of assigning a single line-of-sight velocity to each photon package, photon packages are characterized by a line-of-sight velocity distribution. The combination of this characteristic with the peel-off and forced scattering techniques guarantees that every single photon contributes several times to the observed kinematics at all possible line-of-sight velocities, such that reliable results can be obtained in a reasonable CPU time. For technical details on the implementation we refer to (6) and (8).

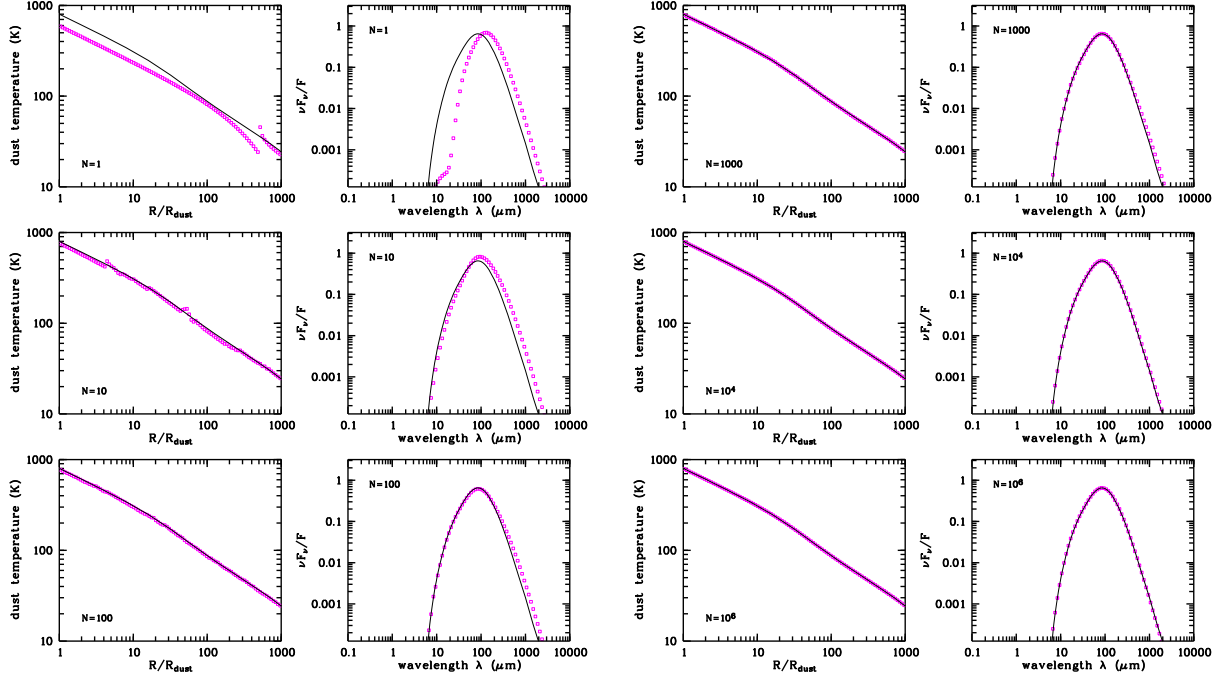


Fig. 1.— Demonstration of the efficiency of the SKIRT code to perform LTE radiative transfer calculations. Shown are the temperature profile (left) and the emerging spectrum (right) as obtained with the SKIRT code for the $p = 0$ and $\tau_V = 100$ benchmark model from Ivezić et al. (26). In each panel, the grey dots are the SKIRT results and the solid black lines represent the benchmark solution. The six simulations presented correspond to the same model, but the number of photon packages in the simulation ranges from 1 (top left) to 10^6 (bottom right). Even with very few photon packages, SKIRT is able to provide good results, thanks to the polychromatic nature of the photon packages.

5. Benchmark results

The only way to test the correct behaviour of a radiative transfer code is by comparing its results with those of other codes on a single well-defined benchmark model. Ivezić et al. (26) provide the first benchmark solution for a continuum LTE radiative transfer model. Their model consists of a single star surrounded by a spherical dusty envelope with optical depths ranging from $\tau_V = 1$ to $\tau_V = 1000$. We have calculated the dust temperature distribution and the emerging spectrum of this benchmark model using the SKIRT code in both spherical and axisymmetric geometries. The agreement with the benchmark results, both for the temperature distribution and the spectral energy distribution, is excellent, for all optical depths. In figure 1 we compare one benchmark model with the results of SKIRT simulation with different numbers of photon packages. Thanks to the polychromatic nature of the photon packages, decent results are already obtained with very

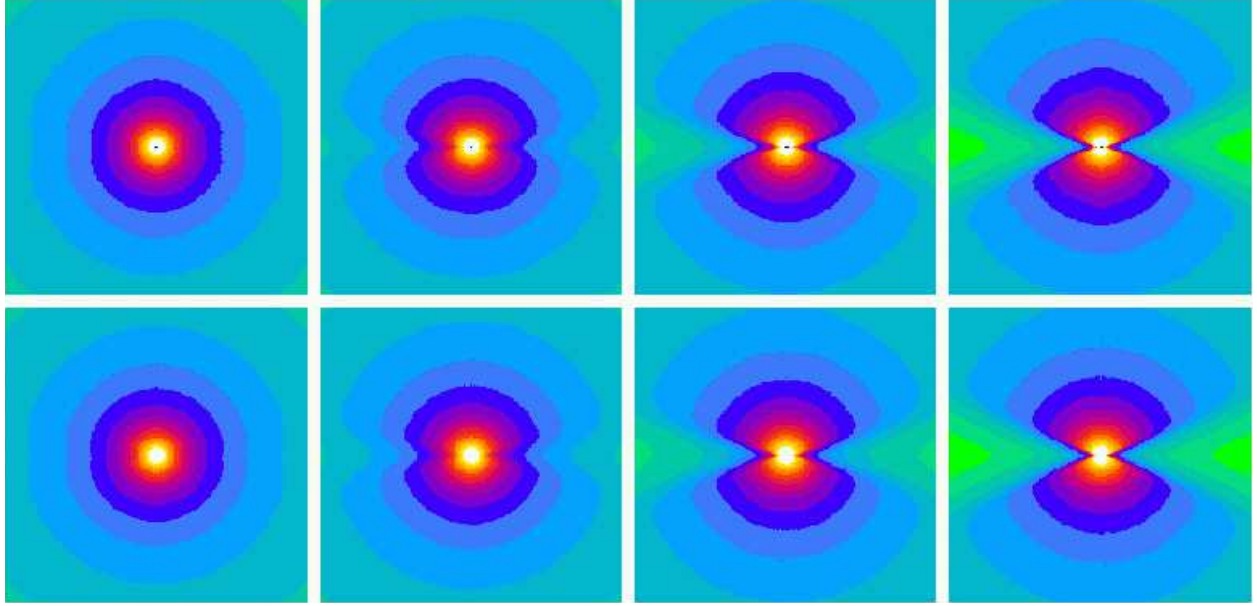


Fig. 2.— SKIRT benchmark tests for the 2D axisymmetric benchmark models from Pascucci et al. (36). The top panels shows the temperature maps of the central 100×100 AU for the models corresponding to $\tau_V = 0.1, 1, 10$ and 100 (from left to right), as obtained with RADICAL. The bottom panels show the corresponding temperature maps obtained with SKIRT with 10^6 photon packages. The agreement is very satisfactory and lies within the uncertainties quoted in (36).

few photon packages. Recently, Pascucci et al. (36) provided a more challenging axisymmetric benchmark model, consisting of a star surrounded by an dusty accretion disk with strong density gradients and optical depths ranging from $\tau_V = 0.1$ to $\tau_V = 100$. They calculated temperature maps and SEDs for these models using five different codes, and found agreement to within some 10 percent. In figure 2 we compare the temperature maps obtained with SKIRT to those obtained with RADICAL, one of the radiative transfer codes used in the benchmark calculations. The agreement between the results is obvious, both for small and large optical depths. The SKIRT simulations to obtain these results took only some 3 hours on a single processor PC.

6. Application 1: Edge-on spiral galaxy SEDs

During the last decade of the past century there has been a vivid discussion about the opacity of spiral galaxies. This discussion was initiated by Disney (19) and Valentijn (42), who countered the conventional view that spiral galaxies are optically thin over their entire optical discs. The most reliable technique to model the dust content of spiral galaxies is to combine imaging and spectra at wavelengths ranging from the optical to the submillimeter. In particular, optical and near-infrared data can be used to model the dust absorption and scattering, whereas FIR/submm maps directly show the thermal emission from the dust. Most of the detailed modelling efforts

have concentrated on nearby edge-on galaxies, where the appearance of a clear dust lane in the optical images puts tight constraints on the dust (e.g. (28), (48), (49), (50), (1), (37), (31), (33), (38)). The number of galaxies for which such studies have been performed is still rather modest however. We are planning to perform a multiwavelength study of a sample of edge-on galaxies in order to investigate the dust distribution, optical depth, stellar SEDs and star formation of spiral galaxies as a function of Hubble type and surface brightness class. We hope to achieve this goal by simultaneous modelling of the optical/NIR images and FIR/submm maps or fluxes with the SKIRT code. An example of the output of the SKIRT code is provided in figure 3, which shows simulated maps of an edge-on galaxy at optical, NIR, FIR and submillimeter wavelengths. Our goal is to fit such maps to the observed data and determine the model parameters using non-linear optimization algorithms. Our first test results using genetic algorithms are promising.

7. Application 2: Elliptical galaxies kinematics

During the past few years, a consensus has developed that elliptical galaxies, like spiral galaxies, contain dark halos. Stellar kinematics are generally considered as the most important tracer for these halos at a few effective radii. Several authors have adopted stellar kinematics to constrain the dark matter distribution in a number of elliptical galaxies ((39), (23)). A possible caveat in these studies is the effect of dust attenuation. Estimates based on IRAS data suggested dust masses in ellipticals of the order of 10^5 to 10^6 M_\odot (25), but more recent ISO, SCUBA and NOBA data increased typical dust mass estimates to about 10^7 M_\odot ((41), (29), (44)).

We have done an extensive investigation of the effects of dust attenuation on the observed kinematics of elliptical galaxies ((2), (7), (5), (6)). For a simple elliptical galaxy model with a smooth dust component with optical depth around unity, the effect of dust attenuation on the observed kinematics is illustrated in figure 4. For the lines of sight that pass near the galaxy center, the kinematics are only slightly affected. At large projected radii, however, the kinematics are seriously affected: the velocity dispersion profile drops less steeply, and the Gauss-Hermite h_4 parameter (a measure for the shape of the line profiles) is significantly larger compared to the dust-free case. These effects are caused by photons emitted by high-velocity stars in the center of the galaxy, that are scattered in the outskirts of the galaxy into lines of sight with a large projected radii. Curiously, these effects are strikingly similar to the kinematical signature of a dark halo, which is characterized by a slowly decreasing dispersion profile and a positive h_4 profile.

To check this into more detail, we considered our dust-affected kinematics as an observational data set, and modelled it in the usual way, i.e. without taking dust attenuation into account. We found that it was impossible to fit both the photometry and the kinematics with a constant mass-to-light ratio model. A dark matter halo is hence necessary to explain the effects caused by dust attenuation. In the best fitting model with a dark halo, the dark matter contributes roughly a third of the total mass within $1 R_e$, and half of the total mass within the last data point. These results clearly demonstrate that the effects of dust attenuation can mimic the presence of

a dark matter halo. In analogy with the mass-anisotropy degeneracy, we are now faced with a new degeneracy, which could be called the mass-dust degeneracy. The new mass-dust degeneracy strongly complicates the use of stellar kinematics as a tracer for the mass distribution in elliptical galaxies: taking dust attenuation into account in dynamical modelling procedures will reduce or may even eliminate the need for a dark matter halo at a few R_e .

8. Application 3: Spiral galaxy rotation curves

The observed flatness of spiral galaxy HI rotation curves out to very large distances clearly demonstrates the presence of dark matter. Less clear, however, is the amount of dark matter present in the inner regions of spiral galaxies. Various authors have reported a discrepancy between the observed shallow slope of dark matter haloes in LSB galaxies and the steep slope predicted by CDM cosmological simulations (e.g. (18), (22)). Important here is that the inner dark matter profiles are usually derived from H α observations, which are subject to dust attenuation.

We have performed radiative transfer simulations with SKIRT to investigate the effect of dust attenuation on the observed (gas and stellar) kinematics of spiral galaxies and to investigate whether dust can serve as a valuable explanation for this discrepancy (8). Figure 5 shows the major and minor axis kinematics (mean projected velocity and velocity dispersion) for a set of spiral galaxy models at various inclinations and with various optical depths. For edge-on galaxies, there is a strong effect of dust attenuation on the observed kinematics. The dispersion profile shows a serious dip in the dust lane, such that stellar kinematics measured through a dust lane should always be treated with much caution. The rotation curve of edge-on spiral galaxies becomes increasingly shallower for increasing optical depths, an effect which is mainly caused by absorption (see also (13), (31), (52)). Edge-on galaxies with an observed shallow rotation curve could hence in reality have an intrinsically steep cusp. However, this effect is strongly reduced when the galaxies are more than a few degrees from exactly edge-on. For inclinations as large as 80 degrees, dust attenuation is completely negligible. On the one hand, this means that inclined galaxies form the ideal targets for stellar kinematical studies, in particular to constrain the mass structure and to study the kinematical history of disc galaxies. On the other hand, it also means that dust attenuation cannot be invoked as a possible mechanism to reconcile the discrepancies between the observed shallow slopes of LSB galaxy rotation curves and the dark matter cusps found in CDM cosmological simulations.

REFERENCES

- Alton P. B., Xilouris E. M., Bianchi S., Davies J., Kylafis N., 2000, A&A, 356, 795
- Baes M., Dejonghe H., 2000, MNRAS, 313, 153
- Baes M., Dejonghe H., 2001, MNRAS, 326, 722

Baes M., Dejonghe H., 2001, MNRAS, 326, 733

Baes M., Dejonghe H., 2001, ApJ, 563, L19

Baes M., Dejonghe H., 2002, MNRAS, 335, 441

Baes M., Dejonghe H., De Rijcke S., 2000, MNRAS, 318, 798

Baes M., et al., 2003, MNRAS, 343, 1081

Baes M., et al., 2004, NewA, submitted

Bianchi S., Davies J. I., Alton P. B., 2000, A&A, 359, 65

Bianchi S., Ferrara A., Giovanardi C., 1996, ApJ, 465, 127

Bjorkman J. E., Wood K., 2001, ApJ, 554, 615

Bosma A., Byun Y., Freeman K. C., Athanassoula E., 1992, ApJ, 400, L21

Bruzual A. G., Magris G., Calvet N., 1988, ApJ, 333, 673

Byun Y. I., Freeman K. C., Kylafis N. D., 1994, ApJ, 432, 114

Cashwell E. D., Everett C. J., 1959, A Practical Manual on the Monte Carlo Method for Random Walk Problems, Pergamon, New York

Davies J. I., 1990, MNRAS, 245, 350

de Blok W. J. G., Bosma A., McGaugh S., 2003, MNRAS, 340, 657

Disney M., Davies J., Phillipps S., 1989, MNRAS, 239, 939

Fischer O., Henning T., Yorke H. W., 1994, A&A, 284, 187

Galliano F., et al., 2003, A&A, 407, 159

Gentile G., Salucci P., Klein U., Vergani D., Kalberla P., 2004, MNRAS, 351, 903

Gerhard O., Jeske G., Saglia R. P., Bender R., 1998, MNRAS, 295, 197

Gordon K. D., Misselt K. A., Witt A. N., Clayton G. C., 2001, ApJ, 551, 269

Goudfrooij P., de Jong T., 1995, A&A, 298, 784

Ivezić Ž., Groenewegen M. A. T., Men'shchikov A., Szczerba R., 1997, MNRAS, 291, 121

Krügel E., Siebenmorgen R., 1994, A&A, 282, 407

Kylafis N. D., Bahcall J. N., 1987, ApJ, 317, 637

Leeuw L. L., Sansom A. E., Robson E. I., Haas M., Kuno N., 2004, *ApJ*, 612, 837

Lucy L. B., 1999, *A&A*, 344, 282

Matthews L. D., Wood K., 2001, *ApJ*, 548, 150

Mattila K., 1970, *A&A*, 9, 53

Misiriotis A., Popescu C. C., Tuffs R., Kylafis N. D., 2001, *A&A*, 372, 775

Misselt K. A., Gordon K. D., Clayton G. C., Wolff M. J., 2001, *ApJ*, 551, 277

Niccolini G., Woitke P., Lopez B., 2003, *A&A*, 399, 703

Pascucci I., et al., 2004, *A&A*, 417, 793

Popescu C. C., Misiriotis A., Kylafis N. D., Tuffs R. J., Fischer J., 2000, *A&A*, 362, 138

Popescu C. C., Tuffs R. J., Kylafis N. D., Madore B. F., 2004, *A&A*, 414, 45

Rix H., de Zeeuw P. T., Cretton N., van der Marel R. P., Carollo C. M., 1997, *ApJ*, 488, 702

Silva L., Granato G. L., Bressan A., Danese L., 1998, *ApJ*, 509, 103

Temi P., Brighenti F., Mathews W. G., Bregman J. D., 2004, *ApJS*, 151, 237

Valentijn E. A., 1990, *Nature*, 346, 153

Valotto C., Giovanelli R., 2004, *AJ*, 128, 115

Vlahakis C., Dunne L., Eales S., 2004, *ESA Conference Series*, SP-577, 79

Wise M. W., Silva D. R., 1996, *ApJ*, 461, 155

Witt A. N., 1977, *ApJS*, 35, 1

Witt A. N., Thronson H. A., Capuano J. M., 1992, *ApJ*, 393, 611

Xilouris E. M., Kylafis N. D., Papamastorakis J., Paleologou E. V., Haerendel G., 1997, *A&A*, 325, 135

Xilouris E. M., Alton P. B., Davies J. I., Kylafis N. D., Papamastorakis J., Trewella M., 1998, *A&A*, 331, 894

Xilouris E. M., Byun Y. I., Kylafis N. D., Paleologou E. V., Papamastorakis J., 1999, *A&A*, 344, 868

Yusef-Zadeh F., Morris M., White R. L., 1984, *ApJ*, 278, 186

Zasov A. V., Khoperskov A. V., 2003, *AstL*, 29, 437

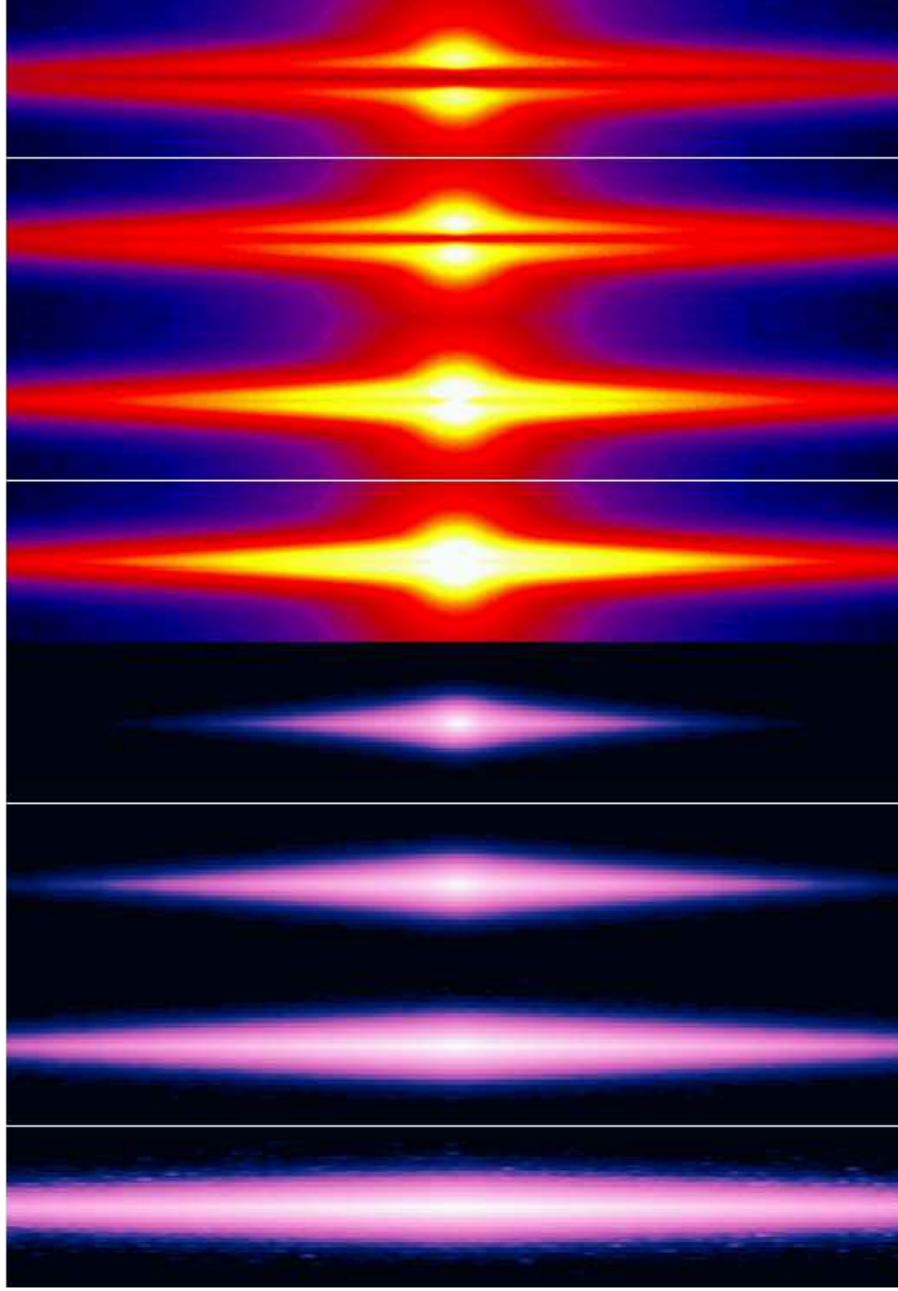


Fig. 3.— Simulated maps of an edge-on spiral galaxy model similar to NGC 891 at various wavelengths ranging from the optical to the submillimeter (from top to bottom: B, I, H, K, 60 μ m, 100 μ m, 200 μ m and 850 μ m). The maps are created by SKIRT from a model including an double exponential disk and a de Vaucouleurs bulge with typical stellar SEDs generated with the PÉGASE stellar population synthesis models. The dust is distributed in an exponential disk with a scale-length $h_d = 1.4 h_*$, a scaleheight $z_d = 0.6 z_*$ and a face-on optical depth $\tau_V = 0.9$. The effects of absorption, scattering and re-emission are properly taken into account.

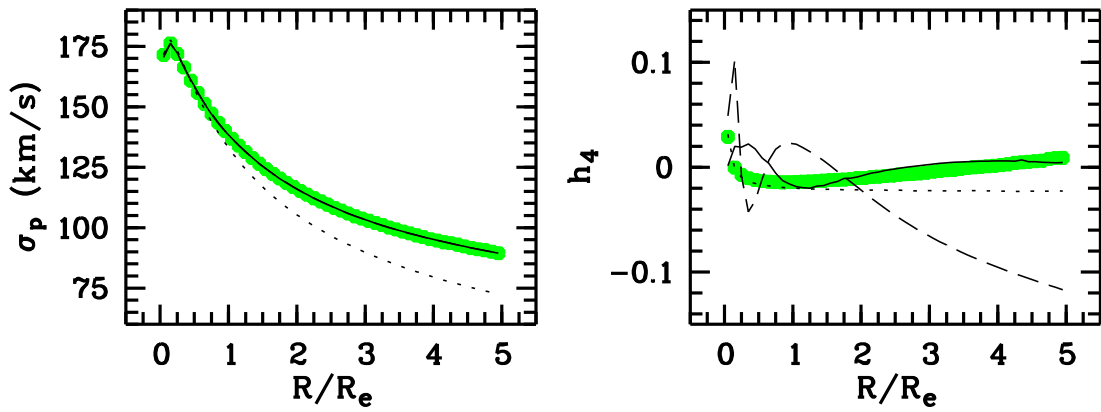


Fig. 4.— The projected dispersion profile and the Gauss-Hermite h_4 profile for a simple dusty elliptical galaxy model with an optical depth $\tau_V = 1$. The dotted lines and the thick grey lines represent the projected kinematics of the input model, respectively without and with dust attenuation taken into account. The latter results are used as input for the dynamical modelling procedure. The dashed lines represent the best fitting model with constant M/L ; the solid line is the best fitting model with a dark matter halo. For more details, see (5).

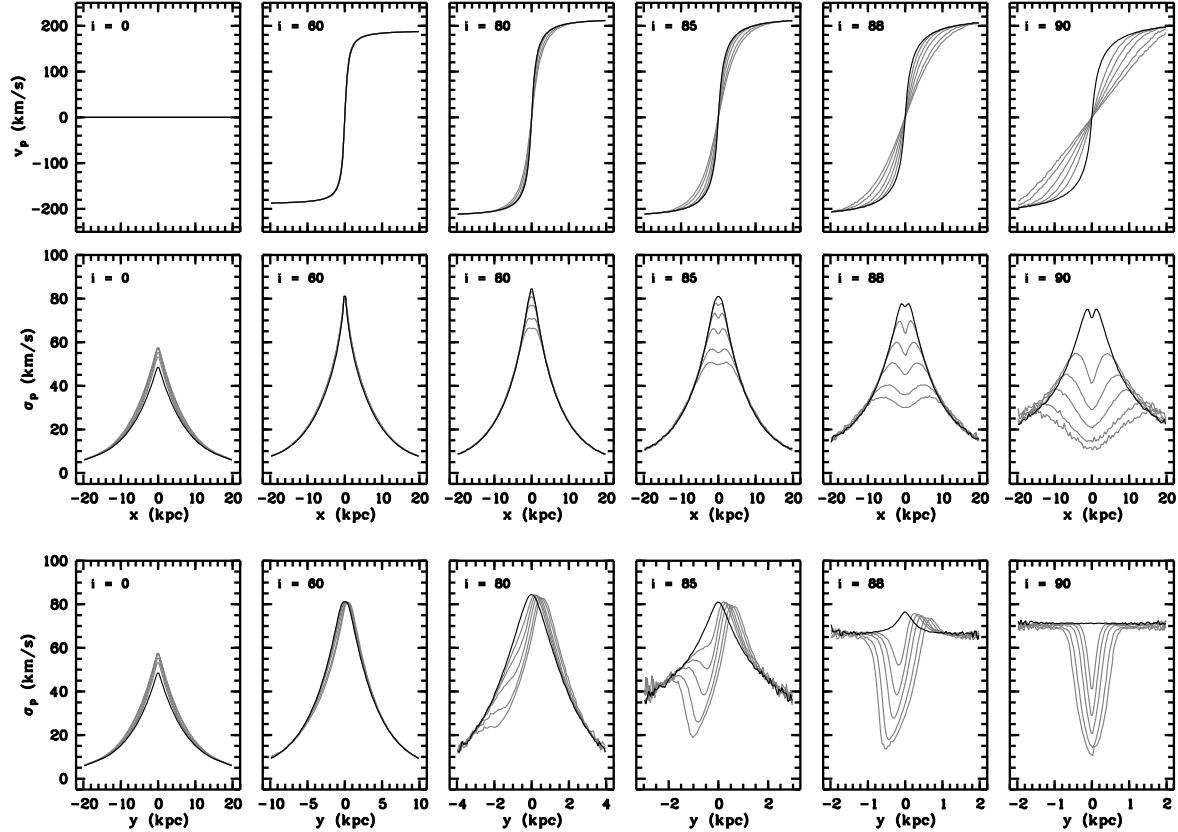


Fig. 5.— The observed kinematics of our galaxy disc models along the major and minor axes. The panels on the two upper rows represent the mean projected velocity profiles and projected velocity dispersion profiles along the major axis, and the bottom row show panels the minor axis projected velocity dispersion profiles. The different columns correspond to inclinations of 0, 60, 80, 85, 88 and 90 degrees (from left to right). The different curves in each panel correspond to different values of the optical depth: models with $\tau_V = 0$ (black), 0.5, 1, 2, 5 and 10 are shown. For more details see (8).